

Photocatalytic three-component asymmetric sulfonylation via direct C(sp³)-H functionalization

Shi Cao¹, Wei Hong¹, Ziqi Ye¹ & Lei Gong¹  [✉]

The direct and selective C(sp³)-H functionalization of cycloalkanes and alkanes is a highly useful process in organic synthesis owing to the low-cost starting materials, the high step and atom economy. Its application to asymmetric catalysis, however, has been scarcely explored. Herein, we disclose our effort toward this goal by incorporation of dual asymmetric photocatalysis by a chiral nickel catalyst and a commercially available organophotocatalyst with a radical relay strategy through sulfur dioxide insertion. Such design leads to the development of three-component asymmetric sulfonylation involving direct functionalization of cycloalkanes, alkanes, toluene derivatives or ethers. The photochemical reaction of a C(sp³)-H precursor, a SO₂ surrogate and a common α,β-unsaturated carbonyl compound proceeds smoothly under mild conditions, delivering a wide range of biologically interesting α-C chiral sulfones with high regio- and enantioselectivity (>50 examples, up to >50:1 rr and 95% ee). This method is applicable to late-stage functionalization of bioactive molecules, and provides an appealing access to enantioenriched compounds starting from the abundant hydrocarbon compounds.

¹Key Laboratory of Chemical Biology of Fujian Province, iChEM, College of Chemistry and Chemical Engineering, Xiamen University, Xiamen, Fujian, China.
✉email: gongl@xmu.edu.cn

Chiral sulfones are building blocks found in many biologically active compounds and drugs¹, and sulfones bearing stereocenters at the α -position or β -position have shown great potential in pharmaceutical and clinical applications (Fig. 1a)^{2–4}. For example, remikiren is a renin inhibitor used for the treatment of hypertension⁵, apremilast has been approved by Food and Drug Administration (FDA) as an oral drug to treat active psoriatic arthritis and plaque psoriasis⁶. Chiral sulfones play important roles in organic synthesis as auxiliaries, ligands, and synthetic intermediates^{7,8}. Great efforts have been devoted to the development of the practical synthesis of enantioenriched sulfones⁹. However, there are few asymmetric catalytic approaches to chiral sulfones with α -carbon stereocenters, and those typically rely on noble-metal-catalyzed asymmetric hydrogenation. Neighboring sulfonyl groups have the potential to stimulate racemization of the non-quaternary stereocenters, thereby synthetic approaches to such compounds which can be performed under mild conditions are strongly desired^{10–14}.

The direct C(sp³)-H functionalization of cycloalkanes and alkanes is a highly useful process due to the low-cost starting materials, the high step, and atom economy (Fig. 1b)^{15,16}. Methods to control site-selectivity towards C-H bonds at the specific positions of unactivated cycloalkanes or alkanes (without the assistance of any directing group)^{17–30}, at the same time combine with asymmetric catalysis, provide appealing opportunities for the construction of high value-added chiral molecules, but remains a remarkable challenge³¹. In this context, rhodium-carbene-induced C-H insertion has emerged as an elegant strategy for alkylation of primary, secondary, tertiary alkanes, and cycloalkanes, in which chiral dirhodium catalysts with well-designed and tailored ligands are employed for both site recognition and asymmetric induction^{32–37}.

Recently, we found a photocatalytic enantioselective alkylation reaction of *N*-sulfonylimines with benzylic or alkyl C(sp³)-H precursors enabled by copper-based asymmetric catalysis and organophotocatalysis. This radical-mediated method however relies on very specific reaction partners and is extremely ineffective for conversions of cycloalkanes³⁸. Practical methods which can be applied to common substrates are still undeveloped. To achieve this goal, suppression of the side reactions such as self-coupling or elimination of radical intermediates and powerful stereocontrol in the radical process is required. Sulfur dioxide and its surrogates have been recognized as useful acceptors for alkyl or aryl radicals in many thermal and photochemical reactions^{39–46}. The resulting sulfonyl radicals have a longer life time which might be beneficial for asymmetric induction⁴⁷. Hence, we questioned whether incorporation of sulfur dioxide insertion with appropriate dual asymmetric photocatalysis^{48–51} would allow us to find an effective approach for stereoselective transformations starting from most abundant hydrocarbon compounds. On the basis of these considerations, a photocatalytic asymmetric three-component sulfonylation reaction of a cycloalkane (an alkane, a toluene derivative, or an ether), an SO₂ surrogate, and a common Michael acceptor was developed, whose stereochemistry was governed by a nickel catalyst of a well-tailored chiral bisoxazoline ligand. This method provides straightforward and economic access to biologically interesting α -C chiral sulfones (>50 examples, up to 50:1 rr and 95% ee, Fig. 1c).

Results

Reaction development. α,β -Unsaturated carbonyl compounds are one class of common Michael acceptors in organic synthesis. Initially, we chose cyclohexane (**1a**) as the model substrate, α,β -unsaturated carbonyl compound bearing an *N*-acylpyrazole moiety (**2a**) as the reaction partner, 5,7,12,14-pentacenetetrone

(**PC1**) as the hydrogen atom transfer (HAT) photocatalyst^{38,52}, and the bisoxazoline nickel complex generated in situ ([**L1**-Ni]) as the chiral catalyst (Table 1). The reaction of **1a** and **2a** failed to produce an additional product under visible light conditions (entry 1). We next tested several SO₂ surrogates in the photochemical system and found that 1,4-Diazabicyclo[2.2.2]octane-1,4-dium-1,4-disulfinate (DABCO·(SO₂)₂) was the appropriate reaction component (entries 2,3). Under irradiation with a 24 W blue LEDs lamp ($\lambda_{\text{max}} = 455 \text{ nm}$) at 20°C under argon, the reaction of **1a**, **2a**, and DABCO·(SO₂)₂ in dichloroethane delivered the chiral sulfone product (**3a**) in 58% conversion and with only 3% ee (entry 3). α,β -Unsaturated carbonyl substrates bearing a different auxiliary group (*Z*) were examined, and it was found that *N*-acylpyrazole (**2a**) was a suitable substrate (entries 4–7). Other photocatalysts (**PC2–PC4**) failed to catalyze this transformation (entries 8–10). In order to improve the reaction efficiency and enantioselectivity, a range of chiral ligands (**L2–L11**) were screened (entries 11–20). Chiral bis(oxazoline) ligands (**L2–L4**) and a tridentate ligand (**L5**), which have been successfully used for asymmetric induction in some radical-mediated transformations^{53–56}, were found to be ineffective in this photocatalytic reaction (entries 11–14), but replacement of **L1** with an indane-derived BOX ligand (**L6**) led to full conversion and significantly increased enantiomeric excess (82% ee) (entry 15). Based on this observation, we modified this type of ligands and synthesized several sterically more bulky analogs for the creation of a more precise chiral environment (**L7–L9**). One of these, **L7** was identified as the best ligand with regard to the yield and enantioselectivity (86% ee) (entry 16). Finally, the reaction was further improved by reducing the reaction temperature and increasing the loading of chiral catalyst, which provided **3a** with a full conversion and 95% ee (entry 23). The reaction with only 1.0 equiv. of cyclohexane also proceeded smoothly at a lower but reasonable reaction rate (52% conversion within 96 h) and similar enantioselectivity of 93% ee (entry 24). Such conditions would be useful with more expensive C(sp³)-H precursors such as natural products or drug molecules.

Reaction scope investigation. With the optimal reaction conditions in hand, we investigated the substrate scope of this photocatalytic asymmetric three-component sulfonylation reaction (Fig. 2). It was revealed that unsubstituted cycloalkanes such as cyclohexane (**1a**), cyclopentane (**1b**), cycloheptane (**1c**), cyclooctane (**1d**), and cyclododecane (**1e**) were excellent substrates, delivering the chiral sulfone products (**3a–3e**) in 62–74% yield and with 91–95% ee. A trisubstituted cycloalkane, 1,3,5-trimethylcyclohexane (**1f**) exhibited high regioselectivity towards the tertiary C(sp³)-H bonds (>50:1 rr) and provided lower enantioselectivity (78% ee). The observation of high regioselectivity was consistent with an inherent difference of bond dissociation energies (BDEs) of secondary and tertiary C(sp³)-H bonds, as well as stability of the corresponding carbon radicals. The crystal structure of product **3b** revealed the absolute configuration (*R*) of the major enantiomer, and the absolute configuration of the other products was assigned accordingly. Adamantane has a significantly higher 3° C(sp³)-H bond dissociation energy of 99 kcal mol⁻¹ caused by its rigid cage structure, which exceeds the bond dissociation energy of its 2° C(sp³)-H bonds (96 kcal mol⁻¹) and those of most other hydrocarbons⁵⁷. The unusually strong tertiary C(sp³)-H bonds of adamantane-type compounds present a remarkable challenge to their selective tertiary C-H functionalization⁵⁸, but such transformations proceeded very well in our photochemical system. Adamantane (**1g**), 1-methyladamantane (**1h**), 1-ethyladamantane (**1i**), and 1,3-dimethyladamantane (**1j**) were all selectively functionalized at the

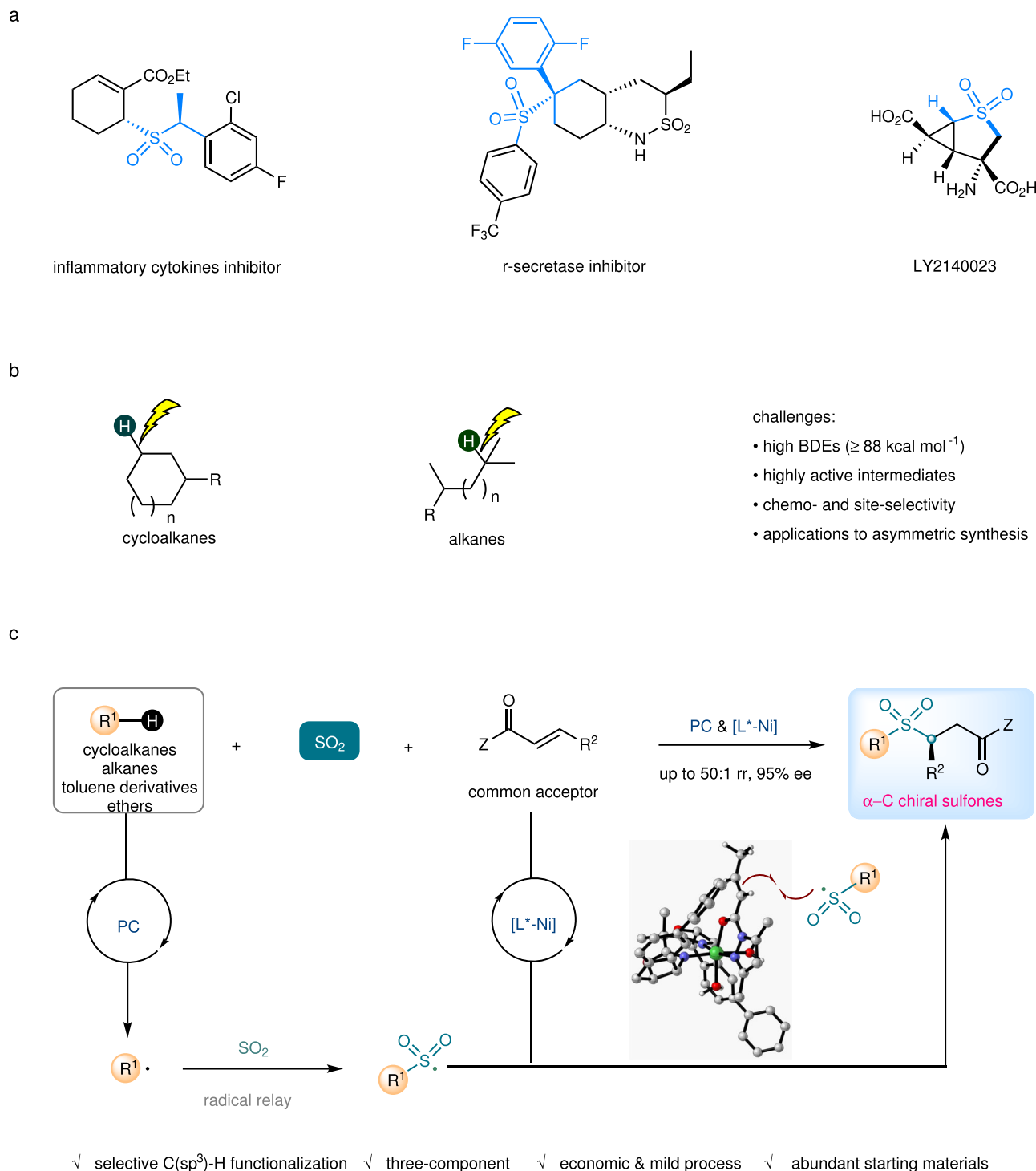
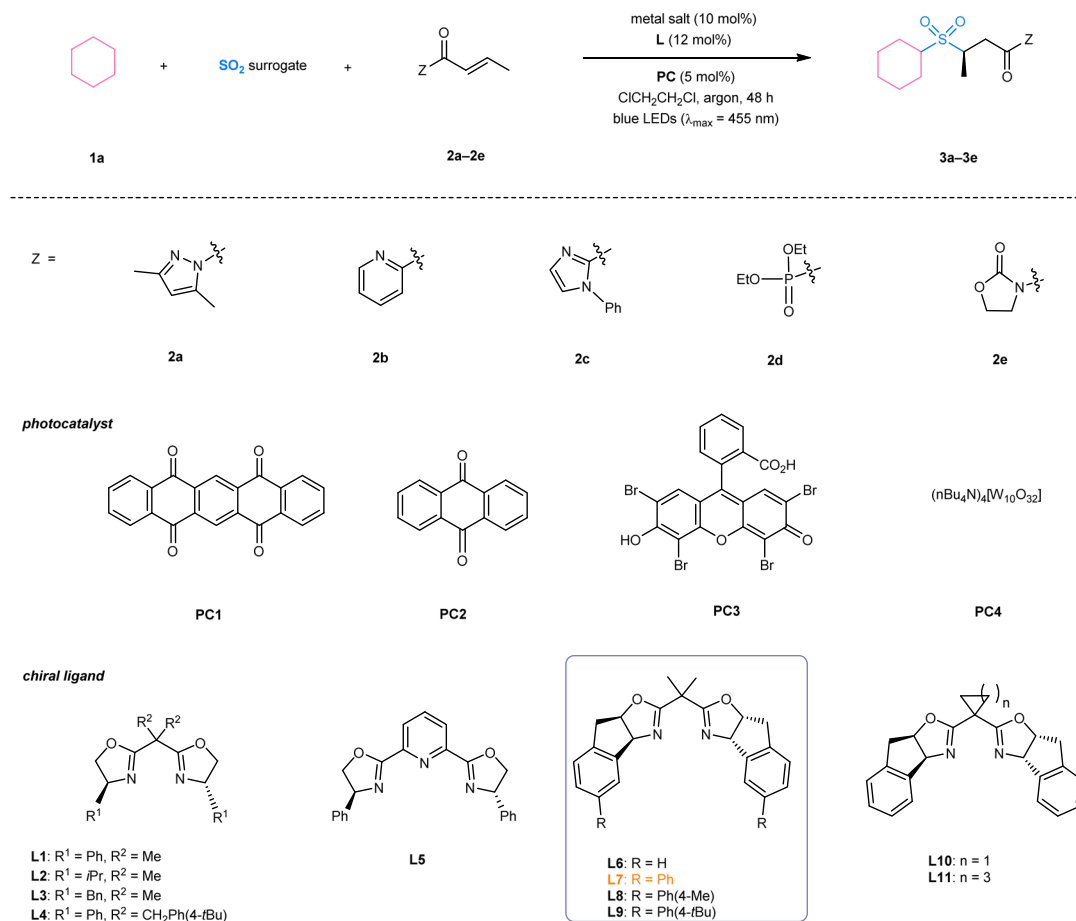


Fig. 1 Overview of this work. **a** Bioactive molecules or natural products containing $\alpha\text{-C}$ chiral sulfone units. **b** Challenges of direct $\text{C}(\text{sp}^3)\text{-H}$ functionalization of cycloalkanes and alkanes. **c** This work: photocatalytic three-component sulfonylation via direct $\text{C}(\text{sp}^3)\text{-H}$ functionalization of cycloalkanes and alkanes. BDEs, bond dissociation energies; rr, regioisomeric ratio; ee, enantiomeric excess; PC, photocatalyst; Z, auxiliary group.

tertiary $\text{C}(\text{sp}^3)\text{-H}$ position, affording the products (**3g–3j**) as single regioisomers with 84–90% ee. These results indicate that the catalyst-control also plays a crucial role in the selectivity in addition to the inherent difference of bond dissociation energies and carbon radical stabilities. The reaction exhibited high functional group compatibility, which would be desirable for its synthetic application to structurally diverse compounds. For example, adamantane derivatives bearing a fluoro- (**1k**), chloro- (**1l**), bromo- (**1m**), cyano- (**1n**), ester- (**1o**), keto- (**1p**), or

hydroxyl- (**1q**) substituent all provided a reasonable yield (59–71%), perfect regioselectivity (>50:1), and satisfactory enantioselectivity (82–91%). Moreover, the photochemical reactions of tertiary alkanes also proceeded smoothly under the standard conditions and delivered the desired chiral sulfones (**3r–3u**) as exclusive regioisomers with 75–82% ee.

To further investigate the generality of this method, other $\text{C}(\text{sp}^3)\text{-H}$ precursors were examined. The reaction with toluene and its derivatives was more rapid than those of cycloalkanes and

Table 1 Optimization of reaction conditions^a.

Entry	Metal salt	Ligand	PC	SO ₂ surrogates	Substrate	T (°C)	Product	Conv. (%) ^b	Ee (%) ^c
1	Ni(ClO ₄) ₂ • 6H ₂ O	L1	PC1	none	2a	20	-	0	n.a.
2	Ni(ClO ₄) ₂ • 6H ₂ O	L1	PC1	Na ₂ S ₂ O ₅	2a	20	3a	0	n.a.
3	Ni(ClO ₄) ₂ • 6H ₂ O	L1	PC1	DABCO • (SO ₂) ₂	2a	20	3a	58	3
4	Ni(ClO ₄) ₂ • 6H ₂ O	L1	PC1	DABCO • (SO ₂) ₂	2b	20	3b	0	n.a.
5	Ni(ClO ₄) ₂ • 6H ₂ O	L1	PC1	DABCO • (SO ₂) ₂	2c	20	3c	0	n.a.
6	Ni(ClO ₄) ₂ • 6H ₂ O	L1	PC1	DABCO • (SO ₂) ₂	2d	20	3d	0	n.a.
7	Ni(ClO ₄) ₂ • 6H ₂ O	L1	PC1	DABCO • (SO ₂) ₂	2e	20	3e	0	n.a.
8	Ni(ClO ₄) ₂ • 6H ₂ O	L1	PC2	DABCO • (SO ₂) ₂	2a	20	3a	0	n.a.
9	Ni(ClO ₄) ₂ • 6H ₂ O	L1	PC3	DABCO • (SO ₂) ₂	2a	20	3a	0	n.a.
10	Ni(ClO ₄) ₂ • 6H ₂ O	L1	PC4	DABCO • (SO ₂) ₂	2a	20	3a	0	n.a.
11	Ni(ClO ₄) ₂ • 6H ₂ O	L2	PC1	DABCO • (SO ₂) ₂	2a	20	3a	47	13
12	Ni(ClO ₄) ₂ • 6H ₂ O	L3	PC1	DABCO • (SO ₂) ₂	2a	20	3a	53	11
13	Ni(ClO ₄) ₂ • 6H ₂ O	L4	PC1	DABCO • (SO ₂) ₂	2a	20	3a	49	21
14	Ni(ClO ₄) ₂ • 6H ₂ O	L5	PC1	DABCO • (SO ₂) ₂	2a	20	3a	37	11
15	Ni(ClO ₄) ₂ • 6H ₂ O	L6	PC1	DABCO • (SO ₂) ₂	2a	20	3a	quant.	82
16	Ni(ClO ₄) ₂ • 6H ₂ O	L7	PC1	DABCO • (SO ₂) ₂	2a	20	3a	quant.	86
17	Ni(ClO ₄) ₂ • 6H ₂ O	L8	PC1	DABCO • (SO ₂) ₂	2a	20	3a	90	84
18	Ni(ClO ₄) ₂ • 6H ₂ O	L9	PC1	DABCO • (SO ₂) ₂	2a	20	3a	85	86
19	Ni(ClO ₄) ₂ • 6H ₂ O	L10	PC1	DABCO • (SO ₂) ₂	2a	20	3a	quant.	82
20	Ni(ClO ₄) ₂ • 6H ₂ O	L11	PC1	DABCO • (SO ₂) ₂	2a	20	3a	quant.	79
21	Ni(ClO ₄) ₂ • 6H ₂ O	L7	PC1	DABCO • (SO ₂) ₂	2a	0	3a	77	95
22	Ni(ClO ₄) ₂ • 6H ₂ O	L7	PC1	DABCO • (SO ₂) ₂	2a	-20	3a	47	95
23 ^d	Ni(ClO ₄) ₂ • 6H ₂ O	L7	PC1	DABCO • (SO ₂) ₂	2a	0	3a	quant.	95
24 ^e	Ni(ClO ₄) ₂ • 6H ₂ O	L7	PC1	DABCO • (SO ₂) ₂	2a	0	3a	52	93

^aReaction conditions: **1a** (1.0 mmol, 10 equiv.), **2a-2e** (0.10 mmol, 1.0 equiv.), SO₂ surrogate (0.075 mmol, 1.5 equiv.), metal salt (0.010 mmol, 10 mol%), ligand (0.012 mmol, 12 mol%), **PC1-PC4** (0.0050 mmol, 5 mol%), ClCH₂CH₂Cl (4.0 mL), indicated temperature, 24 W blue LEDs lamp ($\lambda_{\text{max}} = 455 \text{ nm}$), under argon, see more details for the screening of nickel salts and solvents in Supplementary Table 1.

^bConversion determined by ¹H-NMR.

^cEe value determined by chiral HPLC.

^dNickel salt (0.015 mmol, 15 mol%), chiral ligand (0.018 mmol, 18 mol%).

^eReaction performed with 1.0 equiv. of cyclohexane within 96 h.

PC photocatalyst, Z auxiliary group, conv. conversion, quant. quantitative conversion, n.a., not applicable, DABCO • (SO₂)₂ 1,4-Diazabicyclo[2.2.2]octane-1,4-dium-1,4-disulfinate.

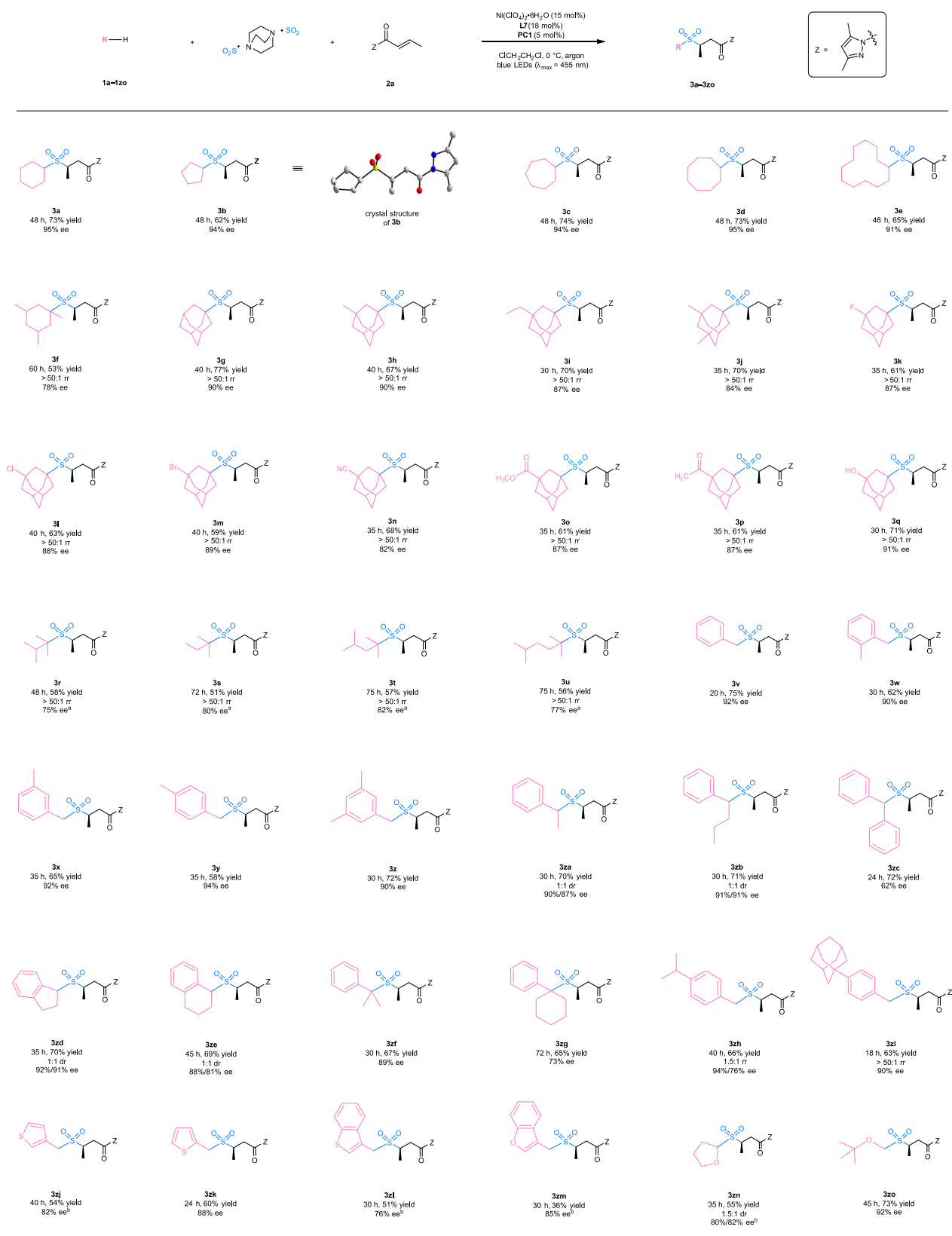


Fig. 2 Reaction scope of C(sp³)-H precursors including cycloalkanes, alkanes, toluene derivatives, and ethers. ^aReaction performed in the presence of alkanes (20 equiv.). ^bReaction performed at 20 °C. PC, photocatalyst; Z, auxiliary group.

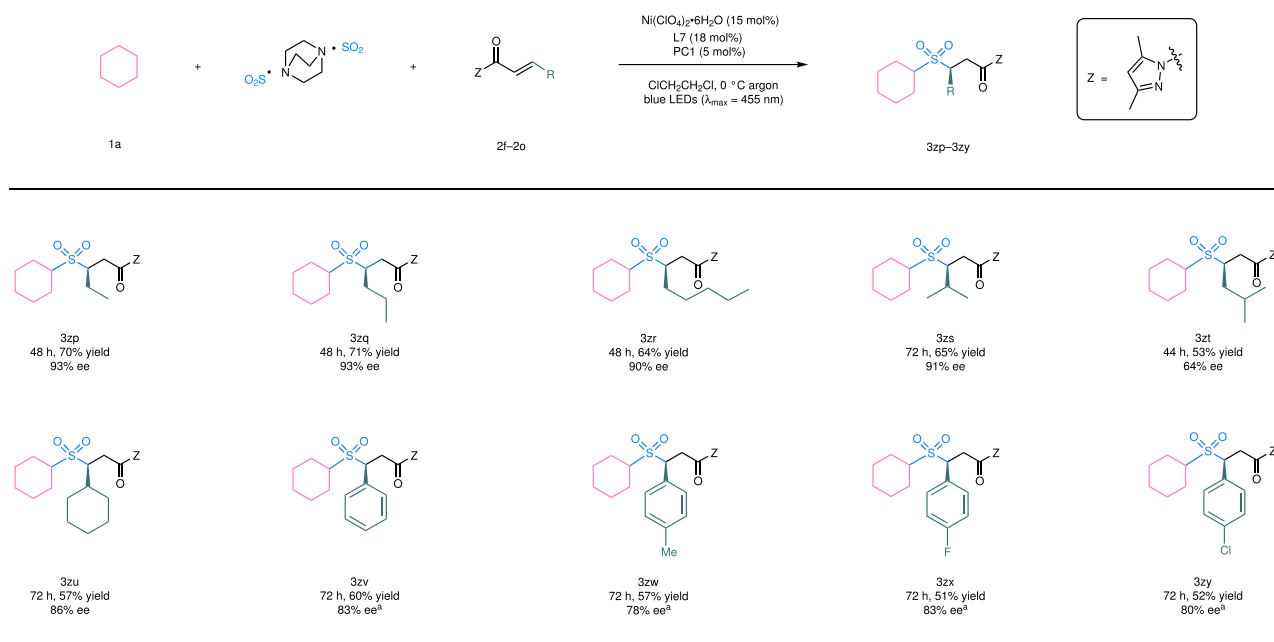


Fig. 3 Reaction scope of α,β -unsaturated *N*-acylpyrazoles. ^aReaction performed at a lower concentration and with a modified substrate ratio, see more details in Supplementary Fig. 1. PC, photocatalyst; Z, auxiliary group.

alkanes. The primary (**1v–1z**), secondary (**1za–1ze**), and tertiary benzylic hydrocarbons (**1zf–1zh**) all worked well and delivered the chiral products (**3v–3zh**) in 58–75% yield and with 62–94% ee. Sterically more demanding substrates such as diphenylmethane (**1zc**) and cyclohexylbenzene (**1zg**) tended to give lower enantioselectivity. The reactions of toluene derivatives containing competing reactive sites displayed some degree of regioselectivity. For example, *p*-isopropyl toluene (**1zh**) provided very moderate regioselectivity of 1.5:1, while 1-(*p*-tolyl)adamantine bearing benzylic C(sp³)-H bonds, secondary and tertiary C(sp³)-H bonds in the adamantyl moiety (**1zi**) afforded a single regioisomer with the benzylic functionalization. It was found that heteroaromatic α -C(sp³)-H precursors such as 3-methylthiophene (**1zj**), 2-methylthiophene (**1zk**), 3-methylbenzothiophene (**1zl**), and 3-methylbenzofuran (**1zm**) were compatible with the reaction and gave products with 76–88% ee. Interestingly, ethers such as tetrahydrofuran (**1zn**) and methyl *tert*-butyl ether (**1zo**), which have strong α -C(sp³)-H bonds (BDEs = ~92 kcal mol⁻¹)⁵⁹, were also identified as excellent substrates by the yields (55–73%) and enantioselectivities (80–92% ee).

We next evaluated the scope of α,β -unsaturated *N*-acylpyrazoles. As summarized in Fig. 3, β -substituents including a linear alkyl group (products **3zp–3zr**), a branched alkyl group (products **3zs, 3zt**), a cycloalkyl group (product **3zu**), and an aryl substituent (products **3zv–3zy**) were all compatible with regards to yields (53–71%) and enantioselectivity (64–93% ee). Typically, β -alkyl-substituted substrates gave better enantioselectivity in comparison to those containing a β -aryl group, perhaps due to the trend of *Z/E* isomerization of the latter under photochemical conditions⁶⁰. For example, in the reaction of **1a** + DABCO·(SO₂)₂ + **2l** → **3zv**, 28% of *Z*-isomer of **2l** was isolated (see more details in Supplementary Fig. 5). Such byproducts were not observed in the conversions of β -alkyl α,β -unsaturated *N*-acylpyrazoles.

Mechanistic studies. Several control experiments were conducted to gain insight into the reaction mechanism (Fig. 4). For example, the addition of a radical quencher (2,2,6,6-tetramethylpiperidine-1-oxyl, TEMPO, 3 equiv.) to the photochemical reaction **1v** +

DABCO·(SO₂)₂ + **2a** → **3v** was found to completely inhibit the transformation to **3v**, instead of affording a TEMPO-carbon radical cross-coupling product (**4**) detected by HRMS analysis. The three-component sulfonylation reaction of 4-(cyclopropylmethyl)-1,1'-biphenyl (**1zp**) under the standard conditions provided a ring-opened product (**5**) in 63% yield and with 95% ee, which further confirmed the reaction pathway via benzylic radicals. Employing cyclopropyl-substituted *N*-acylpyrazole (**2p**) as a substrate for the radical clock experiment provided product **6** in 65% yield and did not give any ring-opened product, thus excluding mechanisms involving the β -carbon radicals of *N*-acylpyrazole complexes⁶¹. The reaction of **2a** with sodium cyclopentanesulfinate was examined under the standard conditions and failed to produce any desired product **3b** (Fig. 4b). This result indicated that the reaction might not proceed through sulfonyl anion intermediates. Moreover, removal of the nickel catalyst in the reaction of **1v** + DABCO·(SO₂)₂ + **2a** → **3v** led to the failure of product formation, while replacing the nickel catalyst with other Lewis acids such as a copper, zinc, iron, or cobalt complex of the same chiral ligand (**L7**) still afforded product **3v** in a moderate yield (17–31%). The cobalt complex with a similar octahedral configuration even gave good enantioselectivity of 80% (Fig. 4c). These results suggested that the nickel complex most likely only provided Lewis acid activation for α,β -unsaturated *N*-acylpyrazoles. Finally, luminescence quenching experiments revealed that the C(sp³)-H precursors such as toluene (**1v**) were capable of quenching the excited state of **PC1** and initiating the radical process (Fig. 4d).

Mechanistic proposal. On the basis of the initial experiments and mechanistic studies, we propose a plausible reaction mechanism (Fig. 5a). The chiral nickel catalyst ([L*·Ni]) undergoes fast ligand exchange with the α,β -unsaturated *N*-acylpyrazole (**2**) to generate an intermediate complex (**A**). On the other hand, the organophotocatalyst (**PC**) is excited to its triplet state (**B**), which performs hydrogen atom abstraction from the C(sp³)-H precursor (**1**) to give the semiquinone-type radical intermediate (**C**) and the transient carbon radical (**D**)⁵². The radical (**D**) is rapidly trapped by the sulfur dioxide released in situ to produce the

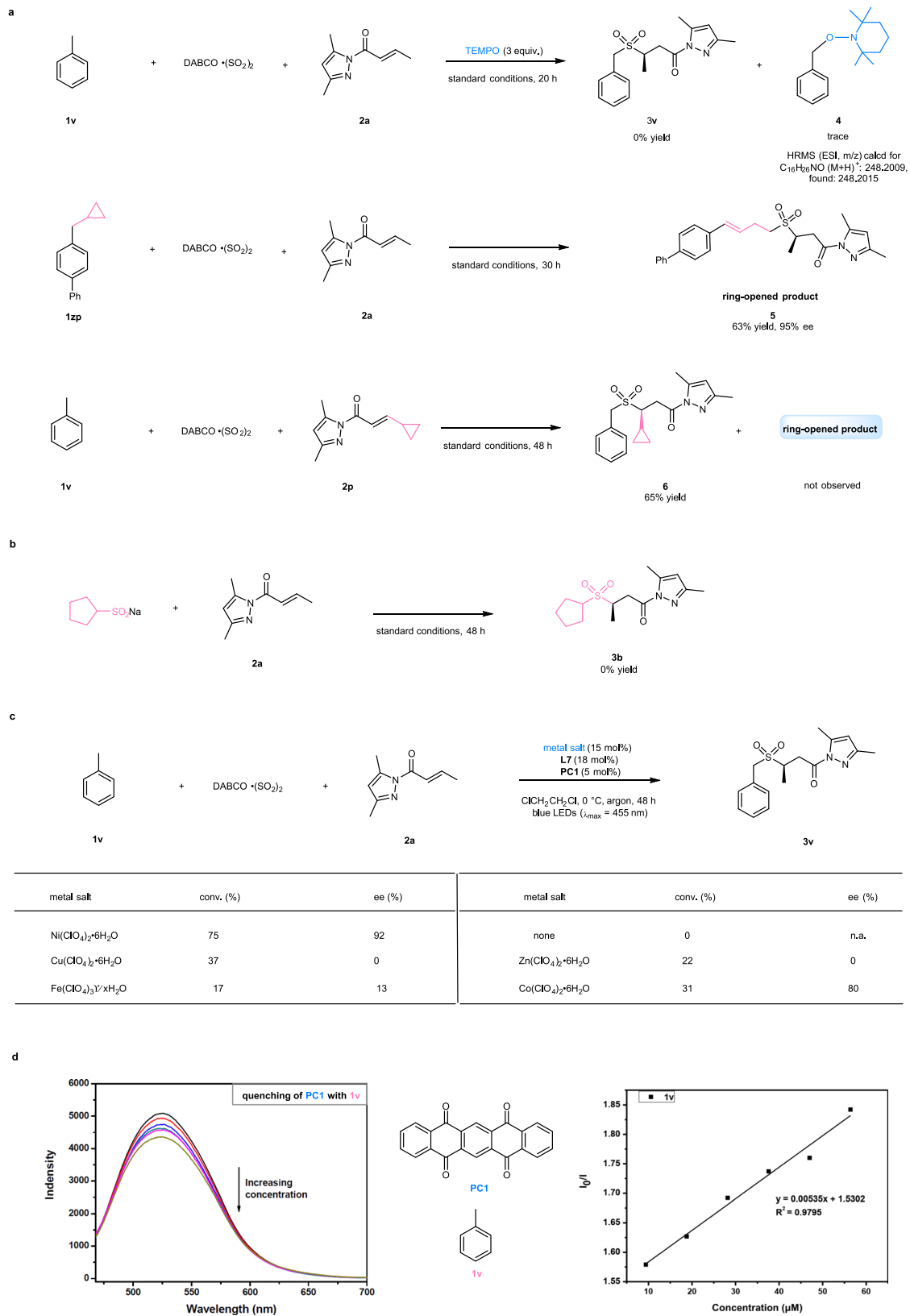


Fig. 4 Control experiments. **a** Probing of carbon radical pathways. **b** Probing of sulfonyl anion pathways. **c** Reactions by other Lewis acids. **d** Luminescence quenching experiments. DABCO • (SO₂)₂, 1,4-Diazabicyclo[2.2.2]octane-1,4-dium-1,4-disulfinate; TEMPO, 2,2,6,6-tetramethylpiperidine-1-oxyl; PC, photocatalyst; equiv., equivalent; conv., conversion; n.a., not applicable.

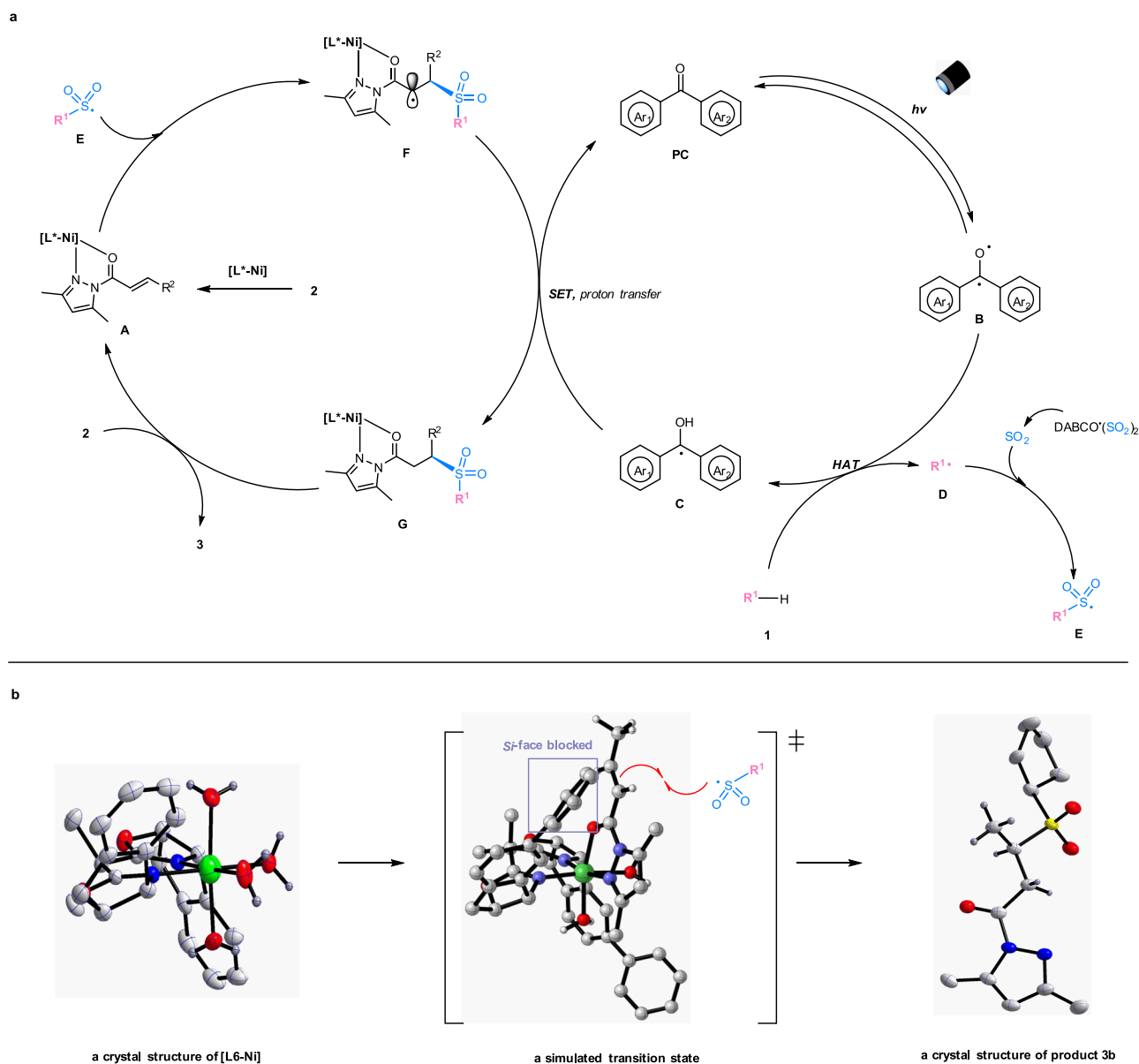


Fig. 5 Proposed reaction mechanism. **a** Proposed catalytic cycles. **b** Left: a crystal structure of chiral nickel complex **[L6-Ni]** (CCDC no. 2054187). Middle: a transition state (**[L7-Ni-2a]** with sulfonamide radical), simulated by Gaussian 09, and drawn by CYLview 1.0. Right: a crystal structure of product **3b** (CCDC no. 2028396). PC, photocatalyst; DABCO • (SO₂)₂, 1,4-Diazabicyclo[2.2.2]octane-1,4-dium-1,4-disulfinate; SET, single electron transfer; HAT, hydrogen atom transfer.

stabilized sulfonamide radical (**E**)⁴¹. Owing to the electronic and steric effects, **E** reacts with the metal-coordinated Michael acceptor (**A**) through an outer-sphere rather than an inner-sphere pathway, affording the radical complex (**F**)^{60,62–66}. Such an outer-sphere attack might be critical to avoid side reactions such as self-coupling or elimination and to achieve a high level of asymmetric induction in the photochemical reaction^{67–80}. Subsequent single electron transfer and proton transfer among intermediates **C**, **F** and a small amount of water in the solution lead to the formation of the neutral complex (**G**) and the organophotocatalyst (**PC**). Ultimately, ligand exchange between intermediate **G** and the substrate (**2**) gives the chiral sulfone product (**3**) and regenerates the coordinated α,β -unsaturated *N*-acylpyrazole (**A**). Besides, a pathway involving DABCO-participated reductive quench cannot be excluded (see more details in the Supplementary Fig. 12)⁵⁸.

A crystal structure of the nickel complex **[L6-Ni]** exhibits an octahedral geometry, in which the six coordination sites are

occupied by one chiral ligand and four water molecules (Fig. 5b, left). Accordingly, an intermediate **[L7-Ni-2a]** is simulated by Gaussian 09, and a proposed transition state is modeled by CYLview 1.0 (Fig. 5b, middle)⁸¹. The sulfonamide radical (**E**) interacts with the C=C double bond of the coordinated α,β -unsaturated *N*-acylpyrazole from *Re*-face with less steric hindrance, which is consistent with an observed *R*-configuration in product **3b** (Fig. 5b, right). The modeled transition state structure also illustrated that the extended phenyl substituents on the chiral ligand (**L7**) were critical for a high level of asymmetric induction.

Synthetic utility. A mmol-scale reaction was performed to demonstrate the synthetic utility of the reaction. A mixture of toluene (**1v**, 533 μ L, 5.0 mmol), **2a** (164 mg, 1.0 mmol) and DABCO • (SO₂)₂ (180 mg, 0.75 mmol) was irradiated with a blue LEDs lamp under the standard conditions (Fig. 6a), leading to the production of 227 mg of **3v** (71% yield, 91% ee). The yield and

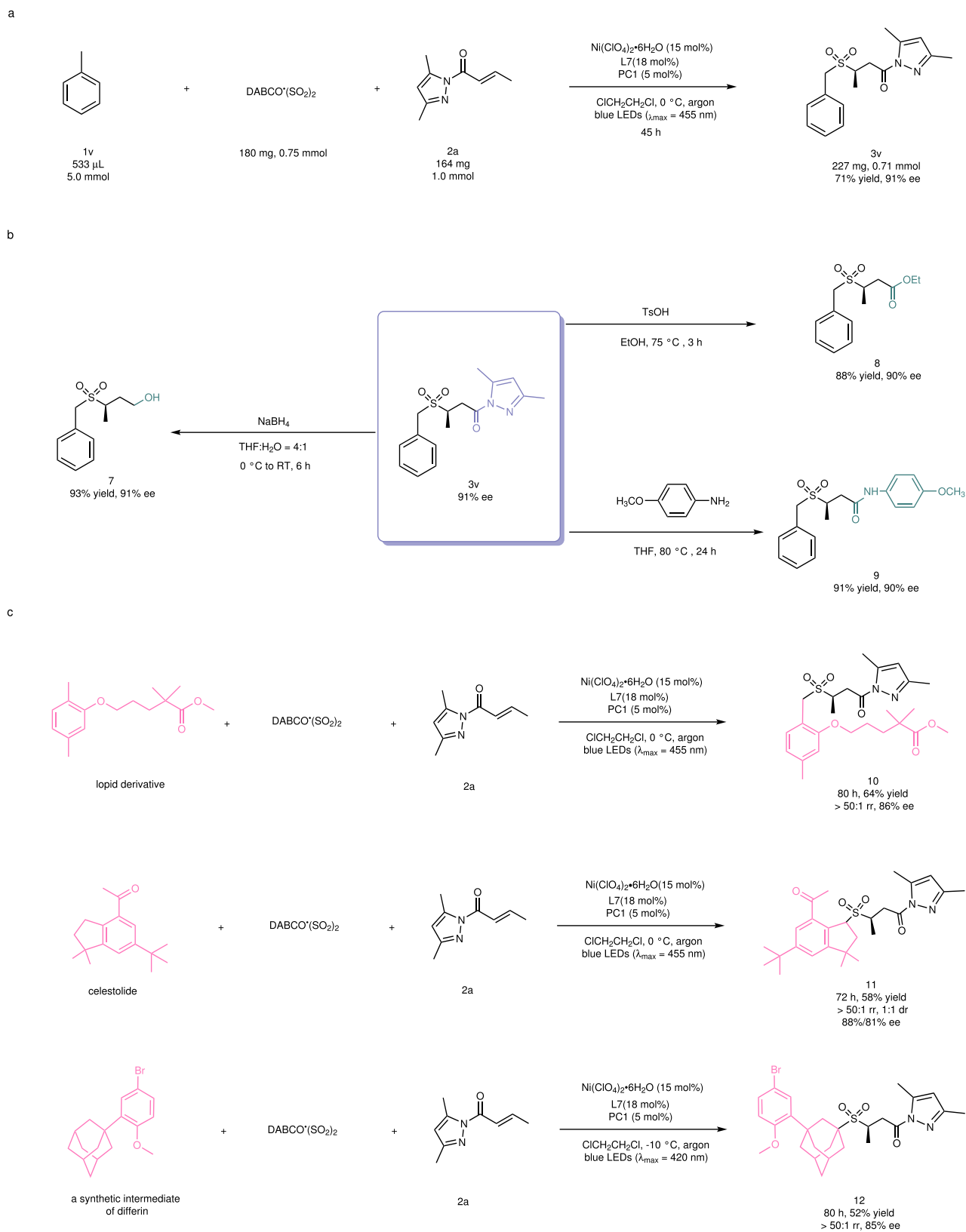


Fig. 6 Synthetic utility of this method. a A mmol-scale photocatalytic reaction. **b** Transformations of chiral sulfone product **3v**. **c** Late-stage modification of bioactive molecules. PC, photocatalyst; DABCO \cdot (SO₂)₂, 1,4-Diazabicyclo[2.2.2]octane-1,4-dium-1,4-disulfinate; THF, tetrahydrofuran; TsOH, 4-Toluenesulfonic acid; RT, room temperature.

enantioselectivity were basically the same as in the small-scale reaction. Next, we investigated further transformations of the reaction product. For example, an alcohol derivative (**7**) was obtained in 93% yield and with 91% ee by treatment of the chiral sulfone (**3v**, 91% ee) with NaBH₄ in a mixed solvent of tetrahydrofuran (THF) and H₂O at 0 °C to room temperature. **3v** could also be converted into the corresponding ester (**8**) or amide (**9**) in good yield and with retention of enantiomeric excess by substitution of the pyrazole moiety with an ethoxy or an amino group, respectively (Fig. 6b). Finally, the photochemical reaction was applied to the late-stage modification of bioactive molecules (Fig. 6c). Under the standard conditions, the reaction of a lipid derivative afforded its chiral sulfone derivative (**10**) as a single regioisomer in 64% yield and with 86% ee. The product was identified by ¹H-NOESY NMR, suggesting that the *ortho*-methyl group was selectively functionalized. We assumed that the excellent site-selectivity towards the C(sp³)-H at the *ortho*-position might be attributed to neighboring electronic effects of the heteroatom (oxygen) and its coordination ability to the nickel catalyst. Such precise recognition of two very similar benzylic C(sp³)-H bonds further confirmed the powerful catalyst-control of selectivity in the photochemical reaction. Using a similar protocol, celestolide and a synthetic intermediate of differin could be converted to the corresponding sulfone products **11** and **12** with excellent regioselectivity and high enantioselectivity, respectively.

Discussion

In summary, we have developed an effective protocol for asymmetric sulfonylation reactions through direct C(sp³)-H functionalization of cycloalkanes, alkanes, toluene derivatives, or ethers. The three-component reaction among an inert C(sp³)-H precursor, an SO₂ surrogate (DABCO·(SO₂)₂), and a common Michael acceptor (α,β-unsaturated carbonyl compound) is enabled by dual organophotocatalysis and nickel-based asymmetric catalysis. A number of biologically interesting enantioenriched α-C sulfones are obtained with high selectivity under mild conditions (> 50 examples, up to 50:1 rr and 95% ee). The SO₂ surrogate provides radical stabilization access for suppression of the side reactions and perhaps being beneficial for stereocontrol in the photochemical reaction. We believe that it would provide an appealing opportunity to develop valuable asymmetric transformations starting from the abundant hydrocarbon compounds.

Methods

Preparation of a solution of the non-racemic nickel catalyst [L7-Ni] in dichloroethane. A solution of Ni(ClO₄)₂·6H₂O (11.0 mg, 0.030 mmol) and non-racemic ligand **L7** (18.4 mg, 0.036 mmol) in 1,2-dimethoxyethane (DME, 4.0 mL) was stirred at 75 °C for 5 h, then the resulting solution was concentrated under reduced pressure to remove the solvent. The residue was redissolved in dichloroethane (DCE, 4.0 mL), which was used freshly as the metal catalyst for the photochemical reactions.

Representative procedure for the photocatalytic asymmetric three-component reaction. A dried 25 mL Schlenk tube was charged with **1a–1zo** (2.0 or 4.0 mmol), **2a** (0.20 mmol), PCI (3.4 mg, 0.010 mmol), DABCO·(SO₂)₂ (36.0 mg, 0.15 mmol), chiral nickel catalyst [L7-Ni] (4.0 mL, taken from the above-mentioned freshly prepared solution in DCE), and DCE (4.0 mL). The mixture was degassed via three freeze-pump-thaw cycles. The Schlenk tube was positioned approximately 5 cm away from a 24 W blue LEDs lamp (λ_{max} = 455 or 420 nm). After being stirred at 0 °C or 20 °C for 24–75 h (monitored by TLC analysis), the reaction mixture was concentrated, then purified by flash chromatography on silica gel (eluted with CH₂Cl₂ or PE:EtOAc = 4:1) to afford a non-racemic product **3a–3zo**, **5–12**.

Data availability

The authors declare that the data supporting the findings of this study are available within this article and its Supplementary Information file, or from the corresponding author upon reasonable request. The experimental procedures and characterization of all

new compounds are provided in Supplementary Information. The X-ray crystallographic coordinates for structures reported in this study have been deposited at the Cambridge Crystallographic Data Centre (CCDC), under deposition numbers CCDC 2028396 (**3b**), and CCDC 2054187 ([L6-Ni]). These data can be obtained free of charge from The Cambridge Crystallographic Data Centre via www.ccdc.cam.ac.uk/data_request/cif.

Received: 13 January 2021; Accepted: 25 March 2021;

Published online: 22 April 2021

References

- Feng, M., Tang, B., Liang, S. H. & Jiang, X. Sulfur containing scaffolds in drugs: synthesis and application in medicinal chemistry. *Curr. Top. Med. Chem.* **16**, 1200–1216 (2016).
- Yamada, M. et al. Novel cyclohexene derivatives as anti-sepsis agents: synthetic studies and inhibition of NO and cytokine production. *Bioorg. Med. Chem.* **16**, 3941–3958 (2008).
- Scott, J. P. et al. Practical asymmetric synthesis of a γ-secretase inhibitor exploiting substrate-controlled intramolecular nitrile oxide-olefin cycloaddition. *J. Org. Chem.* **71**, 3086–3092 (2006).
- Monn, J. A. et al. Synthesis and metabotropic glutamate receptor activity of S-oxidized variants of (–)-4-amino-2-thiabicyclo-[3.1.0]hexane-4,6-dicarboxylate: identification of potent, selective, and orally bioavailable agonists for mGlu2/3 receptors. *J. Med. Chem.* **50**, 233–240 (2007).
- Himmelmann, A., Bergbrant, A., Svensson, A., Hansson, L. & Aurell, M. Remikiren (Ro 42-5892)—an orally active renin inhibitor in essential hypertension: effects on blood pressure and the renin-angiotensin-aldosterone system. *Am. J. Hypertens.* **9**, 517–522 (1996).
- Man, H.-W. et al. Discovery of (S)-N-[2-[1-(3-ethoxy-4-methoxyphenyl)-2-methanesulfonyl]ethyl]-1,3-dioxo-2,3-dihydro-1H-isoindol-4-yl]acetamide (Apremilast), a potent and orally active phosphodiesterase 4 and tumor necrosis factor-α inhibitor. *J. Med. Chem.* **52**, 1522–1524 (2009).
- Alba, A.-N. R., Companyó, X. & Rios, R. Sulfones: new reagents in organocatalysis. *Chem. Soc. Rev.* **39**, 2018–2033 (2010).
- Nielsen, M., Jacobsen, C. B., Holub, N., Paixão, M. W. & Jørgensen, K. A. Asymmetric organocatalysis with sulfones. *Angew. Chem. Int. Ed.* **49**, 2668–2679 (2010).
- Zhang, Z., Butt, N. A. & Zhang, W. Asymmetric hydrogenation of nonaromatic cyclic substrates. *Chem. Rev.* **116**, 14769–14827 (2016).
- Wu, X.-S., Chen, Y., Li, M.-B., Zhou, M.-G. & Tian, S.-K. Direct substitution of primary allylic amines with sulfinate salts. *J. Am. Chem. Soc.* **134**, 14694–14697 (2012).
- Jin, Z., Xu, J., Yang, S., Song, B.-A. & Chi, Y. R. Enantioselective sulfonation of enones with sulfonyl imines by cooperative N-heterocyclic-carbene/thiourea/tertiary-amine multicatalysis. *Angew. Chem. Int. Ed.* **52**, 12354–12358 (2013).
- Yan, Q. et al. Highly efficient enantioselective synthesis of chiral sulfones by Rh-catalyzed asymmetric hydrogenation. *J. Am. Chem. Soc.* **141**, 1749–1756 (2019).
- Cai, A. & Kleij, A. W. Regio- and enantioselective preparation of chiral allylic sulfones featuring elusive quaternary stereocenters. *Angew. Chem. Int. Ed.* **58**, 14944–14949 (2019).
- Zhang, Q., Dong, D. & Zi, W. Palladium-catalyzed regio- and enantioselective hydrosulfonylation of 1,3-dienes with sulfinic acids: scope, mechanism, and origin of selectivity. *J. Am. Chem. Soc.* **142**, 15860–15869 (2020).
- Labinger, J. A. & Bercaw, J. E. Understanding and exploiting C-H bond activation. *Nature* **417**, 507–514 (2002).
- Goldberg, K. I. & Goldman, A. S. Large-scale selective functionalization of alkanes. *Acc. Chem. Res.* **50**, 620–626 (2017).
- Shu, C., Noble, A. & Aggarwal, V. K. Metal-free photoinduced C(sp³)-H borylation of alkanes. *Nature* **586**, 714–719 (2020).
- Shu, W., Lorente, A., Gómez-Bengoa, E. & Nevado, C. Expedient diastereoselective synthesis of elaborated ketones via remote Csp³-H functionalization. *Nat. Commun.* **8**, 13832 (2017).
- Sharma, A. & Hartwig, J. F. Metal-catalysed azidation of tertiary C-H bonds suitable for late-stage functionalization. *Nature* **517**, 600–604 (2015).
- Cook, A. K., Schimler, S. D., Matzger, A. J. & Sanford, M. S. Catalyst-controlled selectivity in the C-H borylation of methane and ethane. *Science* **351**, 1421–1424 (2016).
- Zhang, R. K. et al. Enzymatic assembly of carbon-carbon bonds via iron-catalysed sp³ C-H functionalization. *Nature* **565**, 67–72 (2019).
- Perry, I. B. et al. Direct arylation of strong aliphatic C-H bonds. *Nature* **560**, 70–75 (2018).
- Shu, W. & Nevado, C. Visible-light-mediated remote aliphatic C-H functionalizations through a 1,5-hydrogen transfer cascade. *Angew. Chem. Int. Ed.* **56**, 1881–1884 (2017).

24. Hu, A., Guo, J.-J., Pan, H. & Zuo, Z. Selective functionalization of methane, ethane, and higher alkanes by cerium photocatalysis. *Science* **361**, 668–672 (2018).
25. An, Q. et al. Cerium-catalyzed C-H functionalizations of alkanes utilizing alcohols as hydrogen atom transfer agents. *J. Am. Chem. Soc.* **142**, 6216–6226 (2020).
26. Xu, W., Wang, W., Liu, T., Xie, J. & Zhu, C. Late-stage trifluoromethylthiolation of benzylic C-H bonds. *Nat. Commun.* **10**, 4867 (2019).
27. Ackerman, L. K. G., Martinez Alvarado, J. I. & Doyle, A. G. Direct C-C bond formation from alkanes using Ni-photoredox catalysis. *J. Am. Chem. Soc.* **140**, 14059–14063 (2018).
28. Shen, Y., Gu, Y. & Martin, R. sp^3 C-H arylation and alkylation enabled by the synergy of triplet excited ketones and nickel catalysts. *J. Am. Chem. Soc.* **140**, 12200–12209 (2018).
29. Fan, X.-Z. et al. Eosin Y as a direct hydrogen-atom transfer photocatalyst for the functionalization of C-H bonds. *Angew. Chem. Int. Ed.* **57**, 8514–8518 (2018).
30. Dewanji, A., Krach, P. E. & Rueping, M. The dual role of benzophenone in visible-light/nickel photoredox-catalyzed C-H arylations: hydrogen-atom transfer and energy transfer. *Angew. Chem. Int. Ed.* **58**, 3566–3570 (2019).
31. Davies, H. M. L. & Liao, K. Dirhodium tetracarboxylates as catalysts for selective intermolecular C-H functionalization. *Nat. Rev. Chem.* **3**, 347–360 (2019).
32. Liao, K., Negretti, S., Musaev, D. G., Bacsá, J. & Davies, H. M. L. Site-selective and stereoselective functionalization of unactivated C-H bonds. *Nature* **533**, 230–234 (2016).
33. Liao, K. et al. Site-selective and stereoselective functionalization of non-activated tertiary C-H bonds. *Nature* **551**, 609–613 (2017).
34. Fu, J., Ren, Z., Bacsá, J., Musaev, D. G. & Davies, H. M. L. Desymmetrization of cyclohexanes by site- and stereoselective C-H functionalization. *Nature* **564**, 395–399 (2018).
35. Liao, K. et al. Design of catalysts for site-selective and enantioselective functionalization of non-activated primary C-H bonds. *Nat. Chem.* **10**, 1048–1055 (2018).
36. Garlets, Z. J. et al. Enantioselective C-H functionalization of bicycle[1.1.1] pentanes. *Nat. Catal.* **3**, 351–357 (2020).
37. Garlets, Z. J., Wertz, B. D., Liu, W., Voight, E. A. & Davies, H. M. L. Regio- and stereoselective rhodium(II)-catalyzed C-H functionalization of cyclobutanes. *Chem* **6**, 304–313 (2020).
38. Li, Y., Lei, M. & Gong, L. Photocatalytic regio- and stereoselective $C(sp^3)$ -H functionalization of benzylic and allylic hydrocarbons as well as unactivated alkanes. *Nat. Catal.* **2**, 1016–1026 (2019).
39. Zheng, D., Yu, J. & Wu, J. Generation of sulfonyl radicals from aryldiazonium tetrafluoroborates and sulfur dioxide: the synthesis of 3-sulfonated coumarins. *Angew. Chem. Int. Ed.* **55**, 11925–11929 (2016).
40. Qiu, G., Lai, L., Cheng, J. & Wu, J. Recent advances in sulfonylation reactions of alkenes with the insertion of sulfur dioxide via radical reactions. *Chem. Commun.* **53**, 10405–10414 (2018).
41. Meng, Y., Wang, M. & Jiang, X. Multicomponent reductive cross-coupling of an inorganic sulfur dioxide surrogate: straightforward construction of diversely functionalized sulfones. *Angew. Chem. Int. Ed.* **59**, 1346–1353 (2020).
42. Li, Y., Chen, S., Wang, M. & Jiang, X. Sodium dithionite-mediated decarboxylative sulfonylation: facile access to tertiary sulfones. *Angew. Chem. Int. Ed.* **59**, 8907–8911 (2020).
43. Ye, S., Zheng, D., Wu, J. & Qiu, G. Photoredox-catalyzed sulfonylation of alkyl iodides, sulfur dioxide, and electron-deficient alkenes. *Chem. Commun.* **55**, 2214–2217 (2019).
44. Wang, X., Yang, M., Xie, W., Fan, X. & Wu, J. Photoredox-catalyzed hydrosulfonylation reaction of electron-deficient alkenes with substituted hantzsch esters and sulfur dioxide. *Chem. Commun.* **55**, 6010–6013 (2019).
45. Xiao, X., Xue, J. & Jiang, X. Polysulfurating reagent for unsymmetrical polysulfide construction. *Nat. Commun.* **9**, 2191 (2018).
46. García-Domínguez, A., Müller, S. & Nevado, C. Nickel-catalyzed intermolecular carbosulfonylation of alkynes via sulfonyl radicals. *Angew. Chem. Int. Ed.* **56**, 9949–9952 (2017).
47. Wang, Y. et al. Synthesis of chiral sulfonyl lactones via copper-catalyzed asymmetric radical reaction of DABCO-(SO_2)₂. *Adv. Synth. Catal.* **360**, 1060–1065 (2018).
48. Yoon, T. P. Photochemical stereocontrol using tandem photoredox-chiral Lewis acid catalysis. *Acc. Chem. Res.* **49**, 2307–2315 (2016).
49. Huang, X. & Meggers, E. Asymmetric photocatalysis with bis-cyclometalated rhodium complexes. *Acc. Chem. Res.* **52**, 833–847 (2019).
50. Lipp, A., Badir, S. O. & Molander, G. A. Stereoinduction in metallaphotoredox catalysis. *Angew. Chem. Int. Ed.* **60**, 1714–1726 (2021).
51. Nicewicz, D. A. & MacMillan, D. W. C. Merging photoredox catalysis with organocatalysis: the direct asymmetric alkylation of aldehydes. *Science* **322**, 77–80 (2008).
52. Kamijo, S., Kamijo, K., Maruoka, K. & Murafuji, T. Aryl ketone catalyzed radical allylation of $C(sp^3)$ -H bonds under photoirradiation. *Org. Lett.* **18**, 6516–6519 (2016).
53. Zhou, J. & Tang, Y. The development and application of chiral trisoxazolines in asymmetric catalysis and molecular recognition. *Chem. Soc. Rev.* **34**, 664–676 (2005).
54. Liao, S., Sun, X.-L. & Tang, Y. Side arm strategy for catalyst design: modifying bisoxazolines for remote control of enantioselection and related. *Acc. Chem. Res.* **47**, 2260–2272 (2014).
55. Wang, F., Chen, P. & Liu, G. Copper-catalyzed radical relay for asymmetric radical transformations. *Acc. Chem. Res.* **51**, 2036–2046 (2018).
56. Li, Z.-L., Fang, G.-C., Gu, Q.-S. & Liu, X.-Y. Recent advances in copper-catalyzed radical-involved asymmetric 1,2-difunctionalization of alkenes. *Chem. Soc. Rev.* **49**, 32–48 (2020).
57. Kruppa, G. H. & Beauchamp, J. L. Energetics and structure of the 1- and 2-adamantyl radicals and their corresponding carbonium ions by photoelectron spectroscopy. *J. Am. Chem. Soc.* **108**, 2162–2169 (1986).
58. Yang, H.-B., Fecue, A. & Martin, D. B. C. Catalyst-controlled C-H functionalization of adamantanes using selective H-atom transfer. *ACS Catal.* **9**, 5708–5715 (2019).
59. Jeffrey, J. L., Terrett, J. A. & MacMillan, D. W. C. O-H hydrogen bonding promotes H-atom transfer from α -C-H bonds for C-alkylation of alcohols. *Science* **349**, 1532–1536 (2015).
60. Kuang, Y. et al. Asymmetric synthesis of 1,4-dicarbonyl compounds from aldehydes by hydrogen atom transfer photocatalysis and chiral Lewis acid catalysis. *Angew. Chem. Int. Ed.* **58**, 16859–16863 (2019).
61. Tanaka, T., Hashiguchi, K., Tanaka, T., Yazaki, R. & Ohshima, T. Chemoselective catalytic dehydrogenative cross-coupling of 2-acylimidazoles: mechanistic investigations and synthetic scope. *ACS Catal.* **8**, 8430–8440 (2018).
62. Huo, H. et al. Asymmetric photoredox transition-metal catalysis activated by visible light. *Nature* **515**, 100–103 (2014).
63. Blum, T. R., Miller, Z. D., Bates, D. M., Guzei, I. A. & Yoon, T. P. Enantioselective photochemistry through Lewis acid-catalyzed triplet energy transfer. *Science* **354**, 1391–1395 (2016).
64. Huang, X. et al. Catalytic asymmetric synthesis of a nitrogen heterocycle through stereocontrolled direct photoreaction from electronically excited states. *Nat. Commun.* **8**, 2245 (2017).
65. Han, B., Li, Y., Yu, Y. & Gong, L. Photocatalytic enantioselective α -aminoalkylation of acyclic imine derivatives by a chiral copper catalyst. *Nat. Commun.* **10**, 3804 (2019).
66. Zhang, K. et al. Exploration of a chiral cobalt catalyst for visible-light-induced enantioselective radical conjugated addition. *Angew. Chem. Int. Ed.* **58**, 13375–13379 (2019).
67. Arceo, E., Jurberg, I. D., Álvarez-Fernández, A. & Melchiorre, P. Photochemical activity of a key donor-acceptor complex can drive stereoselective catalytic α -alkylation of aldehydes. *Nat. Chem.* **5**, 750–756 (2013).
68. Alonso, R. & Bach, T. A Chiral thioxanthone as an organocatalyst for enantioselective [2+2] photocycloaddition reactions induced by visible light. *Angew. Chem. Int. Ed.* **53**, 4368–4371 (2014).
69. Ding, W. et al. Bifunctional photocatalysts for enantioselective aerobic oxidation of β -ketoesters. *J. Am. Chem. Soc.* **139**, 63–66 (2017).
70. Silvi, M., Verrier, C., Rey, Y. P., Buzzetti, L. & Melchiorre, P. Visible-light excitation of iminium ions enables the enantioselective catalytic β -alkylation of enals. *Nat. Chem.* **9**, 868–873 (2017).
71. Li, J. et al. Formal enantioconvergent substitution of alkyl halides via catalytic asymmetric photoredox radical coupling. *Nat. Commun.* **9**, 2445 (2018).
72. Li, F. et al. Chiral acid-catalysed enantioselective C-H functionalization of toluene and its derivatives driven by visible light. *Nat. Commun.* **10**, 1774 (2019).
73. Zhang, H.-H., Zhao, J.-J. & Yu, S. Enantioselective allylic alkylation with 4-alkyl-1,4-dihydro-pyridines enabled by photoredox/palladium cocatalysis. *J. Am. Chem. Soc.* **140**, 16914–16919 (2018).
74. Rand, A. W. et al. Dual catalytic platform for enabling sp^3 α -C-H arylation and alkylation of benzamides. *ACS Catal.* **10**, 4671–4676 (2020).
75. Shen, Y., Gu, Y. & Martin, R. sp^3 C-H arylation and alkylation enabled by the synergy of triplet excited ketones and nickel catalysts. *J. Am. Chem. Soc.* **140**, 12200–12209 (2018).
76. Xia, H.-D. et al. Photoinduced copper-catalyzed asymmetric decarboxylative alkylation with terminal alkynes. *Angew. Chem. Int. Ed.* **59**, 16926–16932 (2020).
77. Mitsunuma, H., Tanabe, S., Fuse, H., Ohkubo, K. & Kanai, M. Catalytic asymmetric allylation of aldehydes with alkenes through allylic $C(sp^3)$ -H

- functionalization mediated by organophotoredox and chiral chromium hybrid catalysis. *Chem. Sci.* **10**, 3459–3465 (2019).
78. Tanabe, S., Mitsunuma, H. & Kanai, M. Catalytic allylation of aldehydes using unactivated alkenes. *J. Am. Chem. Soc.* **142**, 12374–12381 (2020).
79. Cheng, X., Lu, H. & Lu, Z. Enantioselective benzylic C-H arylation via photoredox and nickel dual catalysis. *Nat. Commun.* **10**, 3549 (2019).
80. Wang, T. et al. Enantioselective cyanation via radical-mediated C-C single bond cleavage for synthesis of chiral dinitriles. *Nat. Commun.* **10**, 5373 (2019).
81. Legault, C. Y. *CYLview, 1.0b*. Université de Sherbrooke. <http://www.cylview.org> (2009).

Acknowledgements

We gratefully acknowledge funding from the National Natural Science Foundation of China (grant no. 22071209), the Natural Science Foundation of Fujian Province of China (grant no. 2017J06006), and the Fundamental Research Funds for the Central Universities (grant no. 20720190048).

Author contributions

S.C. and L.G. designed and conceived the project. S.C. and W.H. conducted all the synthetic and mechanistic experiments. S.C., W.H., and L.G. analyzed and interpreted the experimental data. Z.Y. designed and performed the theoretical calculations. L.G. prepared the manuscript. S.C. and Z.Y. prepared the Supplementary Information.

Competing interests

The authors declare no competing interests.

Additional information

Supplementary information The online version contains supplementary material available at <https://doi.org/10.1038/s41467-021-22690-3>.

Correspondence and requests for materials should be addressed to L.G.

Peer review information *Nature Communications* thanks the anonymous reviewers for their contribution to the peer review of this work. Peer reviewer reports are available.

Reprints and permission information is available at <http://www.nature.com/reprints>

Publisher's note Springer Nature remains neutral with regard to jurisdictional claims in published maps and institutional affiliations.



Open Access This article is licensed under a Creative Commons Attribution 4.0 International License, which permits use, sharing, adaptation, distribution and reproduction in any medium or format, as long as you give appropriate credit to the original author(s) and the source, provide a link to the Creative Commons license, and indicate if changes were made. The images or other third party material in this article are included in the article's Creative Commons license, unless indicated otherwise in a credit line to the material. If material is not included in the article's Creative Commons license and your intended use is not permitted by statutory regulation or exceeds the permitted use, you will need to obtain permission directly from the copyright holder. To view a copy of this license, visit <http://creativecommons.org/licenses/by/4.0/>.

© The Author(s) 2021